SUPPLEMENTARY DATA

Gene silencing H-NS paralogue StpA forms a rigid protein filament along DNA that blocks DNA accessibility

Ci Ji Lim[1,2,3,4,#], Yixun R. Whang[2,3,4,#], Linda J. Kenney[2,5,6,*] and Jie Yan[1,2,3,4,*]

[1]NUS Graduate school for Integrative Sciences and Engineering, Singapore, 119077; [2]Mechanobiology Institute, National University of Singapore, Singapore, 117411; [3]Centre for Bioimaging Sciences, National University of Singapore, Singapore, 117546; [4]Department of Physics, National University of Singapore, Singapore, 117542; [5]Department of Microbiology & Immunology, University of Illinois at Chicago, Chicago, IL 60612; [6]Department of Biological Sciences, National University of Singapore, Singapore, 117543

[#]These authors contributed equally to this work

[*]Corresponding authors

Jie Yan: phyyj@nus.edu.sg,

Linda J. Kenney: kenneyl@uic.edu

SUPPLEMENTARY METHODS

Over-expression and Purification of E.coli StpA

pET-14b DNA plasmid containing the StpA gene (expressing an N-terminal 6xHis-tagged protein) was transformed into BL21 (DE3) Escherichia Coli cells using standard heat-shock method. The transformed cells were then grown in LB media containing ampicillin at 37 °C to an OD600 of ≈ 0.6-0.7 before IPTG was added to induce StpA expression. After induction, the cells were harvested before going through cell-lysis by sonication. Dnase (RQ1 Dnase, Promega, U.S.A.) was added into

the cell lysate and incubated on ice for at least 3 hours to digest any remaining genomic DNA fragments. The lysate was then centrifuged and the supernatant was collected. The supernatant solution was then adjusted to contain a final concentration of 1 M NaCl and 20 mM immidazole.

StpA was purified using gravity-flow immobilized metal affinity chromatography. Nickel-charged resin (Ni-NTA Agarose, Qiagen, Singapore) was added to bind to the 6xHis-tagged StpA. The sample was placed in a filter column and washed with 10 ml of washing buffer (20 mM immidazole in a 50 mM phosphate, 500 mM NaCl buffer), followed by 1 ml of pre-elution buffer (100 mM immidazole). The protein was then eluted in 2.5 ml of elution buffer (250 mM immidazole). SDS-PAGE was run to determine the purity and molecular weight of the protein, and the protein concentration was measured using Nanodrop ND1000 (Wilmington, U.S.A.). Mass spectroscopy was done to further ensure the desired protein is obtained. Glycerol up to 50% was added before storing in -20 °C. StpA isoelectric point was calculated using pI/MW tool from Expasy website (http://au.expasy.org/tools/pi_tool.html).

Atomic Force Microscopy Imaging and Data Analysis

DNA of two different length were used in imaging: 5,386 bp linearized ϕX174 dsDNA (New England Biolabs) and 576 bp dsDNA constructed by PCR method described previously (1). Long DNA such as λ-DNA are not typically used in AFM due to its length (≈16 μm), which exceeds the scan area of AFM experiments which is only up to 4 μm in order to achieve high-resolution imaging. In experiments, DNA was incubated with StpA and deposited on a glutaraldehyde-coated mica surface for AFM imaging. As shown previously, glutaraldehyde-coated mica surfaces allow DNA-protein complexes to be deposited on the surface in any buffer condition and are able to preserve the conformations of DNA-protein complexes such as nucleosome arrays, DNA-IHF complexes, and DNA-H-NS complexes (2-5). The mica was prepared by depositing 0.1 % APTES solution on a 0.5 cm x 0.5 cm piece of mica for 15 minutes. The mica was then rinsed with deionised water, dried with nitrogen gas before

incubating in a desiccator for at least two hours. Next 1 % glutaraldehyde solution was deposited for 15 minutes and the mica was washed and dried as before. In such method, glutaraldehyde is fixed onto the mica surface and it does not diffuse into solution to cause artificial protein-DNA cross-linking in free solution.

A solution of 0.2 ng/µl linearized ϕX174 DNA with an appropriate concentration of StpA (300 nM for a 1:1 monomer to base pair ratio) was mixed and incubated for 20 minutes. The solution was then deposited on the mica for 20 minutes, following which the mica was washed with 3 millilitres of deionised water and then dried with nitrogen gas. When 576 bp DNA rather than ϕX174 DNA was used, the same protocol was used except that the DNA-StpA reaction mix was diluted once before depositing it on the mica.

Imaging was done using an AFM (5500 AFM, Agilent Technologies, Singapore) in Acoustic AC mode. Sample imaging was done at varying scan size of 1-4 µm square, resolution of 512 x 512 or 1024 x 1024 points and scan speed of 1 line per second. After the AFM is processed with Gwyddion software (http://gwyddion.net/), DNA contour length and end-to-end distance are measured using home-written software written with Matlab (MathWorks, Natick, M.A.). The processed image is further filtered by a mean filter before converting to a binary image with a user-defined threshold value. The digitization of DNA polymer was based on previously described methods (6). The DNA polymer image is digitized by skeletonizing the binary image into single pixel width curved line. Naturally, the single pixel width curved line represents the DNA backbone, connecting through the center of the backbone, see Figure S8.

Since the digitized DNA polymer is a series of eight connected chaincode, length determination can be done by calculating how many even and odd codes and using an estimator to get the final contour length. In our software, the corner chain estimator was used (7). This estimator includes an

additional count, corner count. Every consecutive odd-even or even-odd count is considered a corner count. The contour length of the digitized DNA polymer is then expressed as

$$L_{DNA} = L_{pixel}(0.980n_e + 1.406n_o - 0.091n_c) \quad (1)$$

Where L_{pixel} is the calibrated pixel dimension, n_e is the number of even count, n_o is the number of odd count and n_c is the number of corner count. The end-to-end distance, defined by the distance between the ends of the polymer is calculated by the measuring the distance between the first and last pixel of the digitized DNA polymer.

Transverse Magnetic Tweezers Experiment Setup

The transverse magnetic tweezers setup is similar to the one described in previous work (4,8), see Figure S9. The longer edge of a No. 0 coverslip is polished to achieve a flat surface which is then functionalized with streptavidin. A reaction channel with approximate 150 µl volume is constructed in a way that the polished edge is extended into the centre of the channel. A long DNA (>30,000 bp) construct is optimal for the transverse magnetic tweezers experiment due to the 1-2 µm diffraction shadow on the functionalized coverslip edge. Therefore λ-DNA (48,502 bp, New England Biolabs) was used. Both ends of the λ-DNA were labelled with biotin, forming the DNA construct B-λ-B. Low concentration of the B-λ-B DNA is flushed into the channel and incubated for 10 minutes for one end to bind to the streptavidin-coated coverslip edge. Remaining unbound B-λ-B DNA is then washed before adding in streptavidin-coated magnetic beads (Dynabeads M-280 Streptavidin, Invitrogen, Singapore).

A permanent magnet is then used to apply magnetic force on the tethered magnetic beads. A 50 X microscope objective is used to image the tethered magnetic bead onto a CCD camera (Pike F-032, Allied Vision Technologies, Germany). The image is acquired at 100 frames per second. A home-written software with LabVIEW (National Instruments, US) was used to track the magnetic bead.

Centroid tracking method was applied to obtain the position of the tethered magnetic bead and thus, the DNA extension. The applied magnetic force is calculated using the following equation (9,10):

$$F = \frac{k_B T z}{\langle \delta x^2 \rangle} \qquad (2)$$

Where k_B is the Boltzmann constant, T is temperature, z is the DNA extension and $<\delta x^2>$ is the transverse fluctuation along a direction perpendicular to the direction of force. To ensure if we are stretching a single DNA molecule, the measured DNA force-extension curve is fitted with the Marko-Siggia from the worm-like-chain DNA polymer model, which will give an apparent persistent length value of ≈ 50 ± 5 nm for a single DNA tether in 150 mM KCl and pH 7.5 (11,12). After a single DNA tether is obtained, addition of protein or change of buffer was done using a mechanical syringe pump (NE-1000, New Era Pump Systems, Farmingdale, N.Y.) to minimized perturbations to the DNA measurements.

The force-extension curves of the DNA or DNA-StpA co-filament were fitted with the high-force regime of the Marko-Siggia WLC model (See equation below) using OriginPro 8 (OriginLab, Northampton, MA, US) to obtain the apparent persistence length, A of the polymer. For naked DNA, this equation is valid for applied forces above ≈ 0.08 pN (12). The fitting will contain two variables: apparent persistence length, A and DNA contour length, L.

$$\frac{z}{L} = 1 - \sqrt{\frac{K_B T}{4FA}} \qquad (3)$$

High-throughput Magnetic Tweezers Experiment Setup

For the high-throughput magnetic tweezers experiments to study DNA tethers digestion by DNase I, around 10 DNA tethers are simultaneously monitored at 5 fps using a 10X objective. For the bead attached to each DNA, a small square region of interest (ROI) of a dimension of the bead diameter

was created to enclose the bead. Under a constant force ≈ 3-5 pN, the bead fluctuation is small and its centroid is always inside in the ROI. If the tether is a single DNA, cleaving of the DNA by DNase I results in a free bead moving along the force direction. Once the centroid is outside the ROI, a tether breakage event was recorded. If there are more than one DNA tethers in between the bead and the surface, this method will only record the breakage if the first DNA. This is because the cutting of the first DNA results in greater tension applied to the remaining DNA tethers, resulting in a longer extension. As a result, the bead will also move out of the ROI, and a single breakage event will be recorded in experiments (see Figure S10). In addition, to ensure experimental repeatability, we repeated all high-throughput magnetic tweezers DNase I assays at least twice which allowed us to obtain a rough estimation of the DNA tether lifetime (defined here as time taken for 50% digestion of DNA tethers divided by total DNA tether number) in various buffer conditions. For naked DNA, the values are: 3 ± 1 seconds in 50 mM KCl and 320 nM Dnase I, 8 ± 1 seconds in 500 mM KCl and 1280 nM Dnase I, 6 ± 5 seconds in 50 mM KCl, 10 mM $MgCl_2$ and 32 nM Dnase I.

SUPPLEMENTARY DISCUSSION

DNA bending persistence length and DNA conformation

The bending persistence length (or simply persistence length), A is a parameter that is proportional to the bending rigidity by $A*K_BT$ of a polymer chain (11,12). It is defined as the contour distance where the correlation is negligible between two tangent vectors along the polymer. When the contour length is comparable or shorter than A, the thermal deformation of the polymer can be approximated by a smooth bending into an arc that has a constant curvature. When the two ends of the polymer meets with the same tangential orientation, the polymer will have a smooth circular shape.

In our AFM imaging experiments, it is not clear whether the StpA-DNA complex reaches 2-dimensional equilibrium where the tangent vector correlation function is twice of persistence length

A, or just a 2-dimensional projection of its 3-dimensional conformation where the correlation function is A. When the contour length is larger than the correlation function, the smooth deformation is no longer a good approximation due to the loss of correlation along the longer backbone. When the two ends of such a long polymer meet with the same tangential orientation, the cyclized polymer will be a more random coiled shape instead of a smooth circle.

For a naked DNA, A is around 50 nm in physiological buffer conditions (11-13). The end circles in main article Figure 1A have a minimal contour length of ≈ 200 nm, which is four times larger than the naked DNA persistence length. The fact that these circles are smooth and round suggests that the DNA inside the loops is homogeneously coated with StpA which leads to an increased bending persistence $A_{DNA/StpA\text{-}co\text{-}filament}$ by 2-4 folds depending on whether the conformation on surface is relaxed or is a projection of the 3-d conformation.

More direct evidence is revealed by comparisons between naked linear 576 bp DNA and StpA coated ones (See main article Figure 2 E-H). The distributions of the end-to-end distance divided by the contour length of the two species show that the StpA-coated DNA is straightened to nearly the full contour length, while the naked DNA has a much more flattened distribution due to increased conformational fluctuation of a less rigid backbone.

SUPPLEMENTARY FIGURES

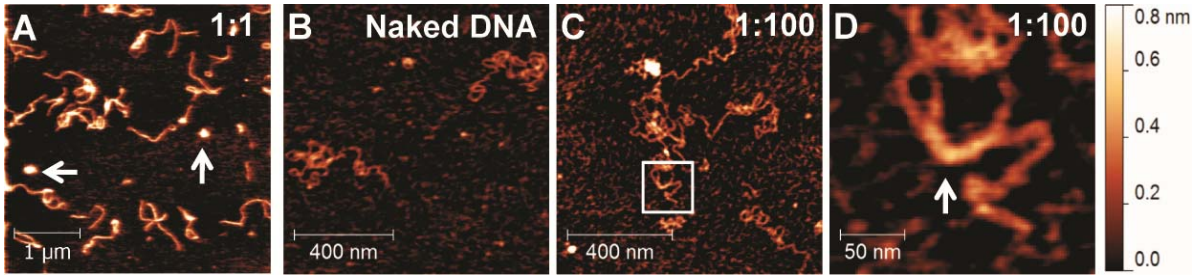

Supplementary Figure S1. AFM images of StpA DNA-bridging capability and the StpA protein filament on DNA is unable to interact with another DNA bound protein filament. All images are done using

the same buffer as Figure 1 containing 50 mM KCl. The StpA/DNA bp ratio is indicated at the top right corner of each subpanel. (A) An overall representation of the various StpA induced DNA organizations. Majority of the complexes are elongated DNA-StpA co-filament with large loops. White arrows indicate small scale aggregations that are a minority of the complexes population. (B) Naked linearized ϕX174 DNA substrates. (C) ϕX174 DNA substrates incubated at 1:100 StpA:DNA ratio (3 nM StpA), demonstrating some StpA-DNA binding. (D) A close-up of the white box in Figure S1b, DNA bridging by StpA is indicated by the white arrow.

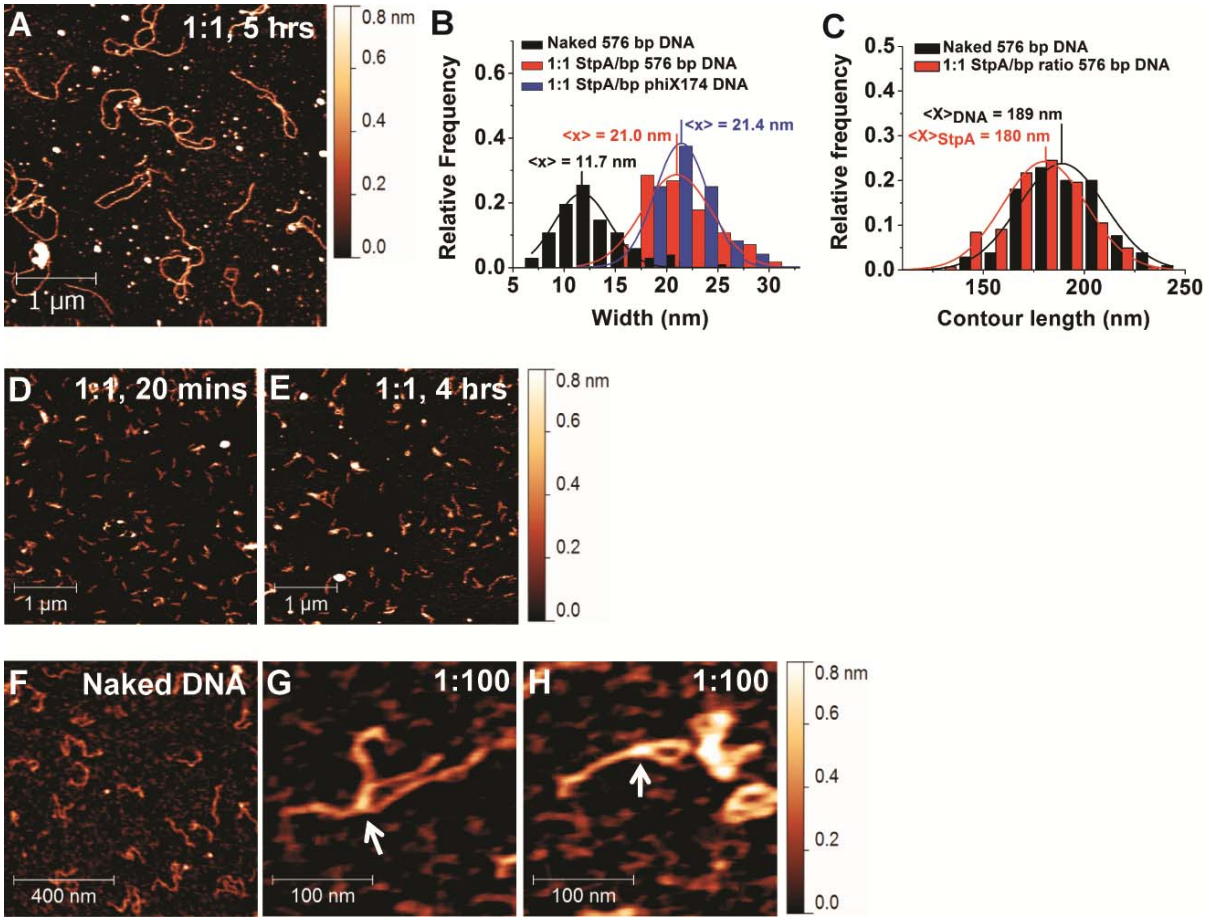

Supplementary Figure S2. AFM images and analysis of DNA-StpA co-filament mediated DNA bridging. The StpA/DNA bp ratio is indicated at the top right corner of each subpanel. (A) ϕX174 DNA incubated at 1:1 StpA:DNA ratio (300 nM StpA) for 5hrs showing no large aggregation that is otherwise predicted by the model in Figure 2A in main article. (B) Width analysis of AFM images of

DNA incubated with/without 1:1 StpA:DNA ratio conditions. It can be seen saturated binding of StpA results in a ~ 10 nm increase in DNA thickness as compared to naked DNA. (C) Contour length analysis of AFM images of 576 bp DNA incubated with/without 1:1 StpA:DNA ratio conditions. There is only a slight reduction in DNA contour length upon saturated StpA binding. (D) 576 bp DNA incubated at 1:1 StpA:DNA ratio for 20 minutes. (E) The same condition incubated for 4 hours before deposition, with no significant difference from (D), suggesting that StpA-coated DNA molecules do not associate with one another. For (D) & (E), 4 x 4 μm images were done to better demonstrate the concentration of the DNA-StpA complexes. (F) Naked linear 576 bp DNA substrates. (G-H) 576 bp DNA substrates incubated at 1:100 StpA:DNA ratio. StpA DNA-bridging events are indicated by white arrows.

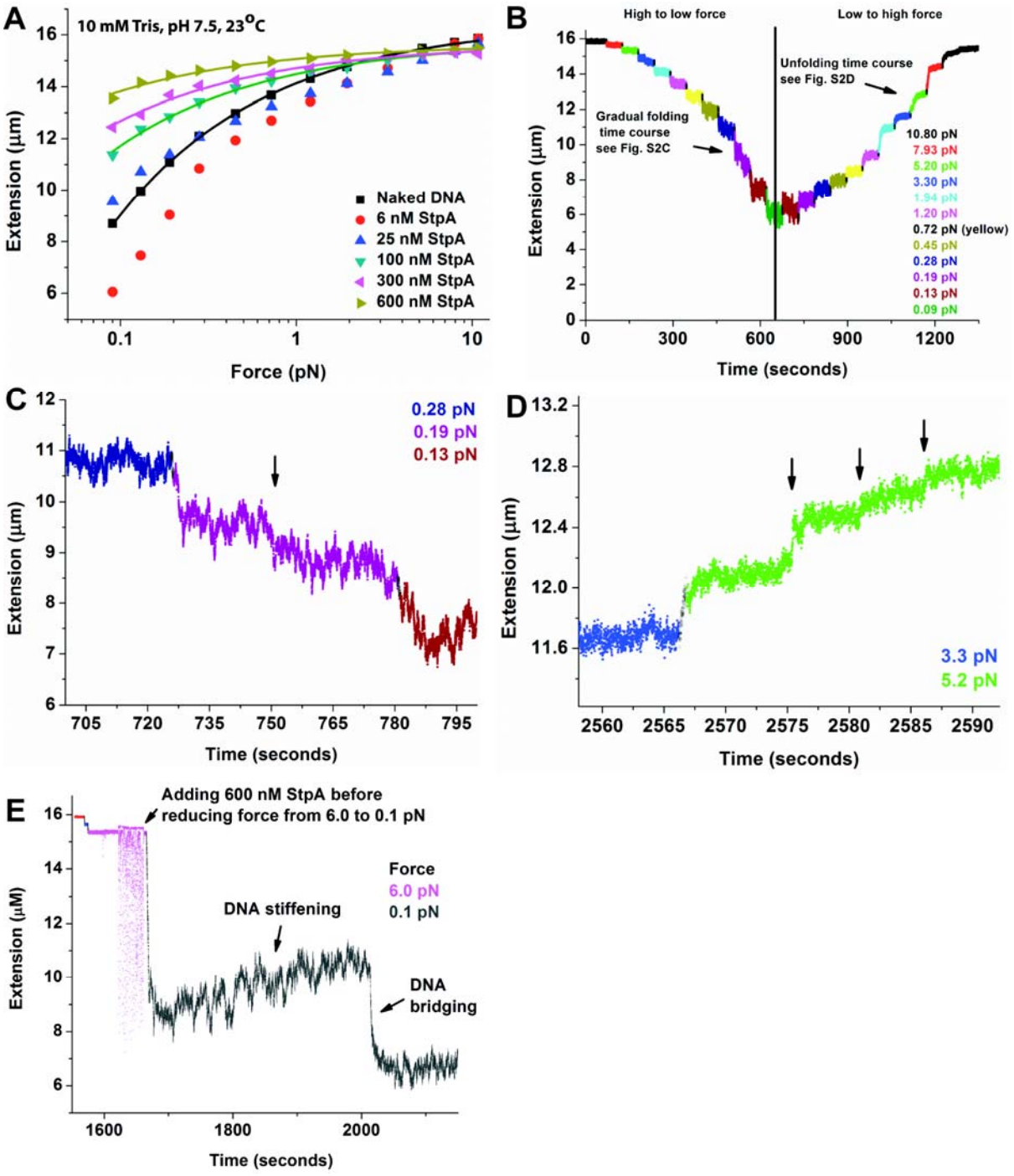

Supplementary Figure S3. Force-extension curves of λ-DNA incubated with varying StpA concentration. (A) Force-extension curves of 6, 25, 100, 300 and 600 nM StpA on the same λ-DNA. Only the forward curves are shown although hysteresis was observed for 6 and 25 nM StpA concentration (see Figure 2A). Marko-Siggia formula from the DNA WLC model was used to fit the 100, 300 and 600 nM StpA experimental data; these are indicated with solid lines of the respective

markers colours. (B) Full time course of 6 nM StpA concentration measurement; from adding protein and starting measurement from high-low force and the reverse. (C) Gradual folding time course at 6 nM StpA concentration. A minor folding event is indicated by the arrow. (D) Unfolding time course of the same concentration and DNA. The unfolding events are indicated by the arrows. (E) Kinetic competition between StpA filament formation on DNA and DNA-StpA co-filament mediated bridging. 600 nM StpA is added rapidly into a new reaction channel before quickly reducing the stretching force from 6 to 0.1 pN to best observe the elongation of DNA extension due to StpA rigid filament formation along DNA. This elongation was followed by an abrupt drop in DNA extension, suggesting DNA-StpA co-filament mediated bridging. This suggests the DNA-StpA co-filament is able to mediate DNA bridges by interacting with naked DNA segments.

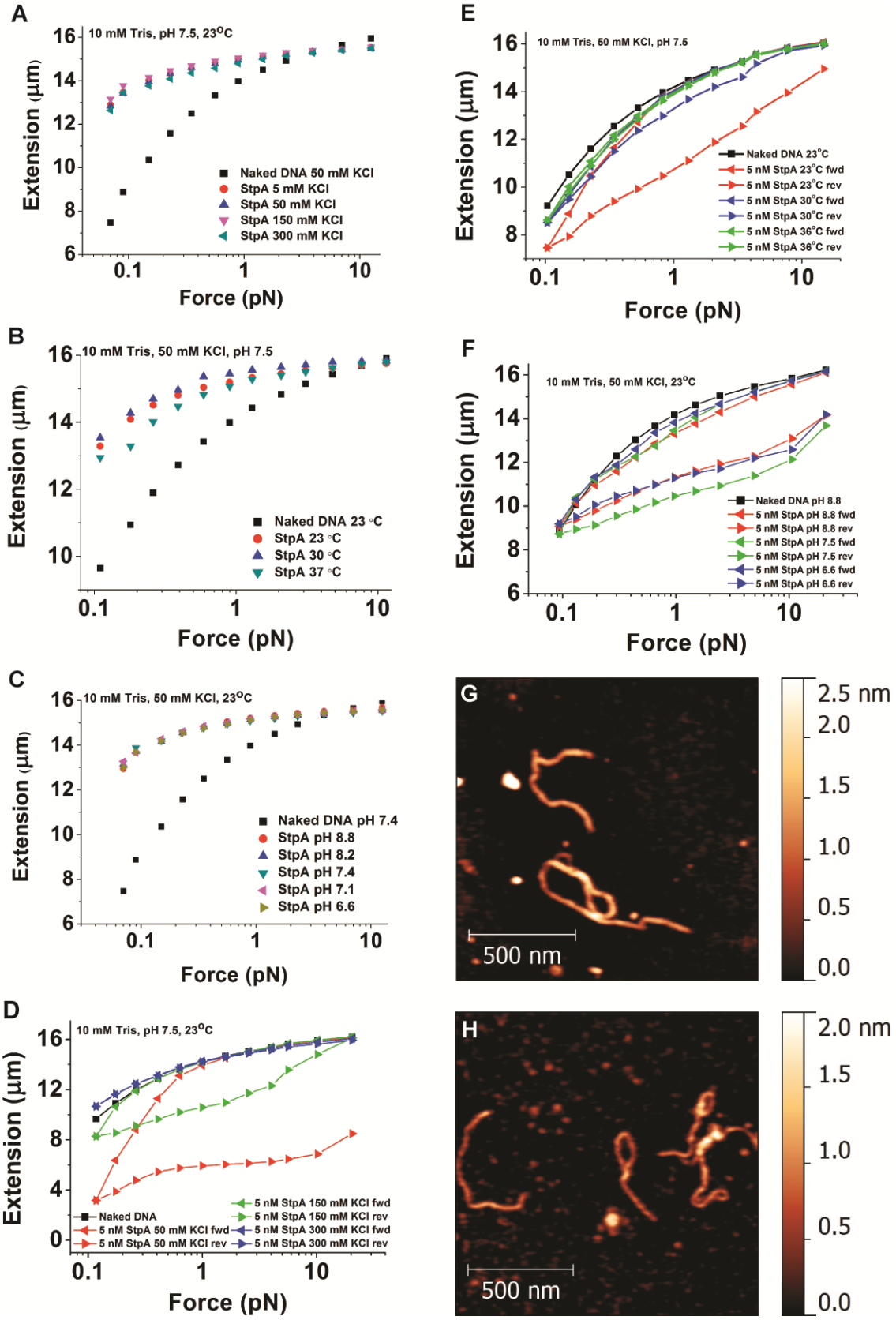
A
10 mM Tris, pH 7.5, 23°C
Extension (µm)
Force (pN)
Naked DNA 50 mM KCl
StpA 5 mM KCl
StpA 50 mM KCl
StpA 150 mM KCl
StpA 300 mM KCl
B
10 mM Tris, 50 mM KCl, pH 7.5
Naked DNA 23 °C
StpA 23 °C
StpA 30 °C
StpA 37 °C
C
10 mM Tris, 50 mM KCl, 23°C
Naked DNA pH 7.4
StpA pH 8.8
StpA pH 8.2
StpA pH 7.4
StpA pH 7.1
StpA pH 6.6
D
10 mM Tris, pH 7.5, 23°C
Naked DNA
5 nM StpA 50 mM KCl fwd
5 nM StpA 50 mM KCl rev
5 nM StpA 150 mM KCl fwd
5 nM StpA 150 mM KCl rev
5 nM StpA 300 mM KCl fwd
5 nM StpA 300 mM KCl rev
E
10 mM Tris, 50 mM KCl, pH 7.5
Naked DNA 23°C
5 nM StpA 23°C fwd
5 nM StpA 23°C rev
5 nM StpA 30°C fwd
5 nM StpA 30°C rev
5 nM StpA 36°C fwd
5 nM StpA 36°C rev
F
10 mM Tris, 50 mM KCl, 23°C
Naked DNA pH 8.8
5 nM StpA pH 8.8 fwd
5 nM StpA pH 8.8 rev
5 nM StpA pH 7.5 fwd
5 nM StpA pH 7.5 rev
5 nM StpA pH 6.6 fwd
5 nM StpA pH 6.6 rev
G
500 nm
2.5 nm
2.0
1.5
1.0
0.5
0.0
H
500 nm
2.0 nm
1.5
1.0
0.5
0.0

Supplementary Figure S4. Single-DNA stretching experiments showing StpA protein filament stability against mono-valent salt, temperature and pH within a physiological range. StpA DNA bridging induced at low StpA concentration is also studied in similar fashion. All experiments were conducted at either 5 or 600 nM StpA, 50 mM KCl, 10 mM Tris buffer pH 7.4 and 23 °C unless stated otherwise. (A) FE curves in 600 nM StpA and 5-300 mM KCl buffer conditions, showing no significant change in binding behaviour with KCl concentration. (B) FE curves in 600 nM StpA and 23-37 °C buffer conditions showing no significant change in binding behaviour with temperature. (C) FE curves in 600 nM StpA and 6.6-8.8 pH buffer conditions, showing no significant change in elastic behaviour with pH, similar to the mono-valent salt and temperature results. (D) FE curves of DNA incubated in 5 nM StpA concentration with increasing KCl. It can be seen as KCl increases, StpA DNA bridging capability is reduced. (E) FE curves of 5 nM StpA with 23-36°C conditions show that at high temperature, StpA induced DNA bridging is also reduced. (F) FE curves of 5 nM StpA with pH 6.6-8.8 show no significant effect on StpA DNA bridging property. (G) AFM images of DNA-StpA complexes at 1:1 StpA/DNA ratio (300 nM StpA) incubated in 150 mM KCl concentration showed formation of rigid DNA-StpA co-filaments. (H) Same as (G) but incubated in 300 mM KCl concentration which showed similar results and is in agreement with single-DNA stretching experimental result in (A) suggesting StpA is able to form rigid filament on DNA up to 300 mM KCl concentration.

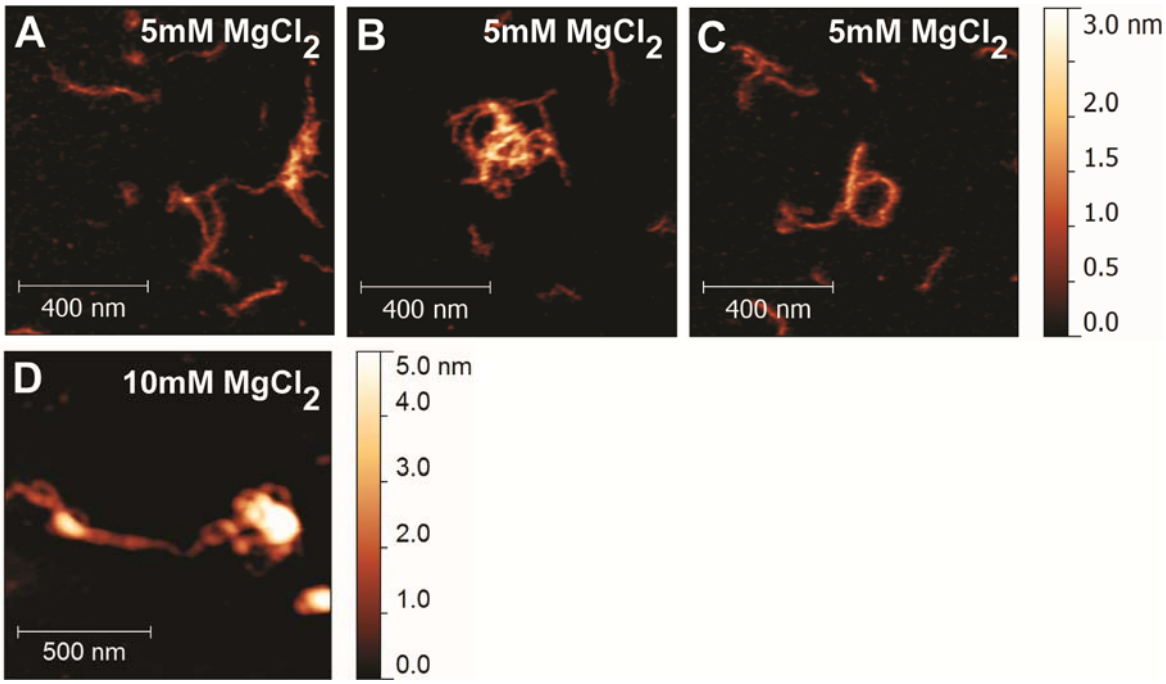

Supplementary Figure S5. Magnesium induced compaction of StpA-coated 576 bp DNA at 5 mM and 10 mM $MgCl_2$ buffer conditions. (A-C) AFM images of linearized 576 bp DNA substrates incubated with 1 StpA per 1 bp ratio (300 nM StpA) at 5 mM $MgCl_2$. It clearly suggests at 5 mM $MgCl_2$, StpA is able to cause fully StpA-coated DNA (DNA-StpA co-filaments) to aggregate via inter-co-filament interactions. (D) Similar experiment but at 10 mM $MgCl_2$ shows the similar trend but at a more drastic effect (See main article Figure 6B & C for similar experiment using a larger DNA substrate).

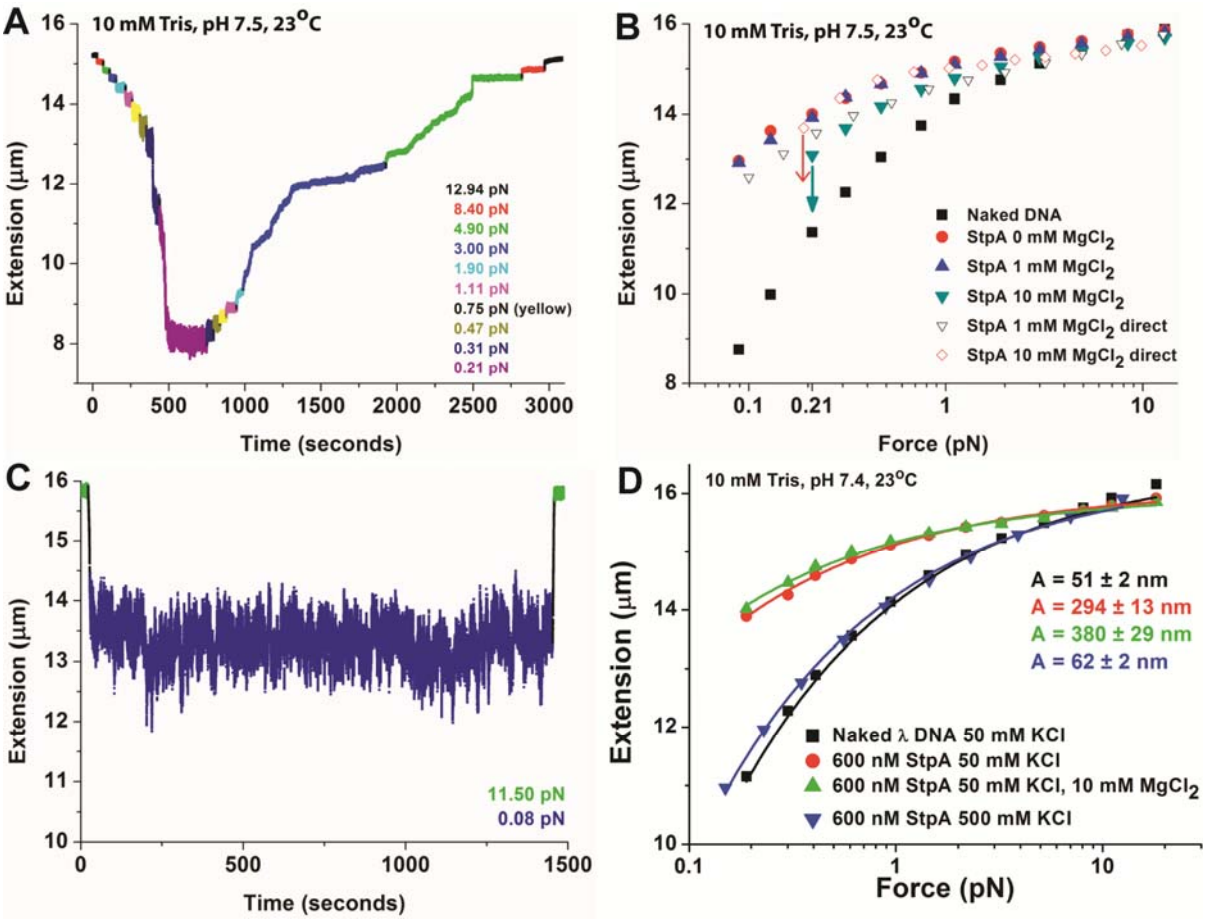

Supplementary Figure S6. Magnesium induced compaction of StpA-coated DNA. (A) Time course of magnesium induced folding at 600 nM StpA in 10 mM $MgCl_2$. The DNA is fully unfolded upon returning back to high force. (B) Single-DNA stretching experiments done when StpA is added in buffer containing 1 mM (Unfilled blue down-triangles) and 10 mM $MgCl_2$ (Unfilled red diamonds, on a different DNA) shows no different from the experiment done by adding StpA at 0 mM $MgCl_2$ and followed by increasing $MgCl_2$ concentration up to 10 mM $MgCl_2$ (Filled markers, done on same DNA). This demonstrates the magnesium induced compaction of StpA-coated DNA is independent of history. (C) Holding the DNA at ≈ 0.1 pN for up to 20 minutes to determine if bound StpA can compact the DNA in buffer containing no magnesium. This was done after the same DNA was compacted in buffer containing magnesium (See main article Figure 6F). (D) To probe the StpA filament persistence length in high magnesium buffer conditions which induces higher order DNA compaction, the time when DNA is held at low force must be minimized as much as possible.

Therefore, we performed force-jumping measurements according to the following protocol. Firstly, the DNA was stretched by 10 pN. Then, the force was quickly jumped to a smaller force and the extension was measured in five seconds. After the extension was measured, the force was jumped back to 10 pN. We found that DNA folding in 5 seconds at low forces was negligible. Applying this method for a range of smaller forces, we were able to obtain the force-extension curve of the StpA-DNA co-filament even in the presence 10 mM $MgCl_2$, which was fitted by the DNA WLC model and got an apparent persistence length value with fitting error of 380 ± 29 nm. When the buffer is switched to 50 mM KCl with no magnesium and no free StpA in solution using the same StpA-coated DNA, an apparent persistence length value with fitting error of 293 ± 13 nm is obtained which is roughly similar to that in the presence of magnesium and also within the standard deviation limit of the statistical obtained value (see main article). In addition, another independent experiment with the DNA incubated with the same StpA concentration but in 500 mM KCl buffer condition, the measured persistence length with fitting error is 62 ± 2 nm which is almost similar to that of a naked DNA. A total of 6 force-jumping measurements yielded a persistence length with statistic standard deviation of 459.31 ± 93.76 nm for 600 nM StpA in 50 mM KCl, 10 mM MgCl2 buffer condition as stated in main article. All fittings have R^2 of >0.98.

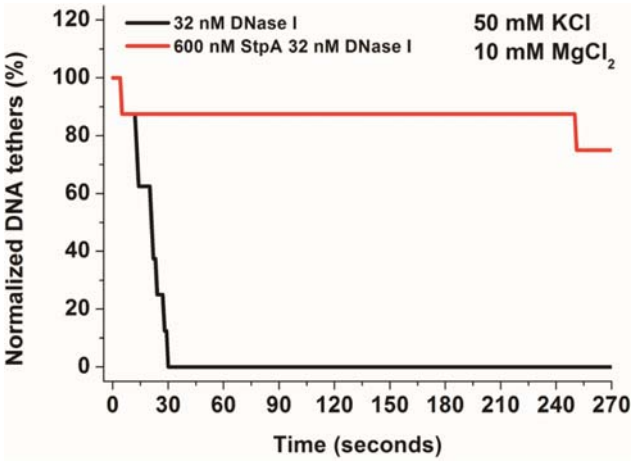

Supplementary Figure S7. StpA protein filament is able to block DNA access in buffer containing 10 mM $MgCl_2$ as demonstrated with a significant reduction in DNase I digestion rate. In presence of magnesium (50 mM KCl, 10 mM $MgCl_2$), StpA is able to form protein filament but is also able to cause DNA compaction (See main article Figure 6E & F). DNase I activity is greatly enhanced in the presence of magnesium therefore a lower concentration is used to achieve the same digestion time scale as previous conditions. In this condition, DNA is protected from DNase I digestion by comparing the red line (600 nM StpA, total 8 DNA tethers) and black line (naked DNA, total 8 DNA tethers). Since DNase I require interaction with DNA for cleavage, it means StpA protein filament is able to block DNA access.

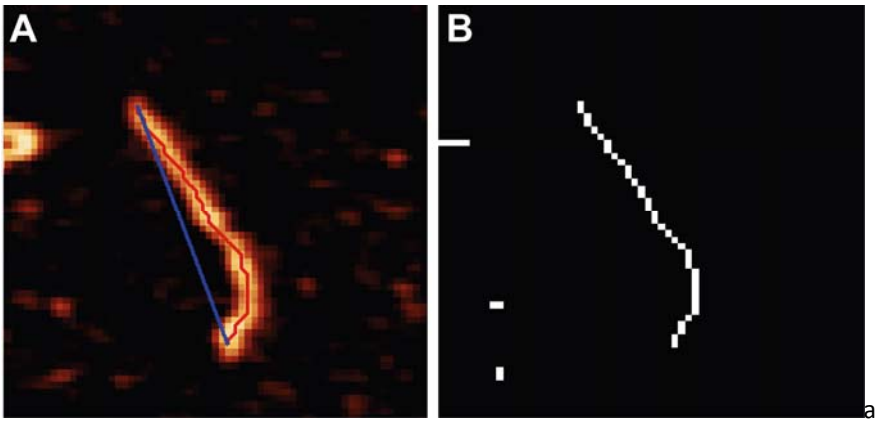

Supplementary Figure S8. DNA contour length and end-to-end distance measurements algorithm. (A) The original processed image with the measured DNA contour length and end-to-end distance

plotted with red and blue line respectively. (B) The digitized binary curved line representing the DNA backbone in the left panel. This is used for performing DNA contour length tracking and end-to-end distance measurement. The scale bar represents 150 nm.

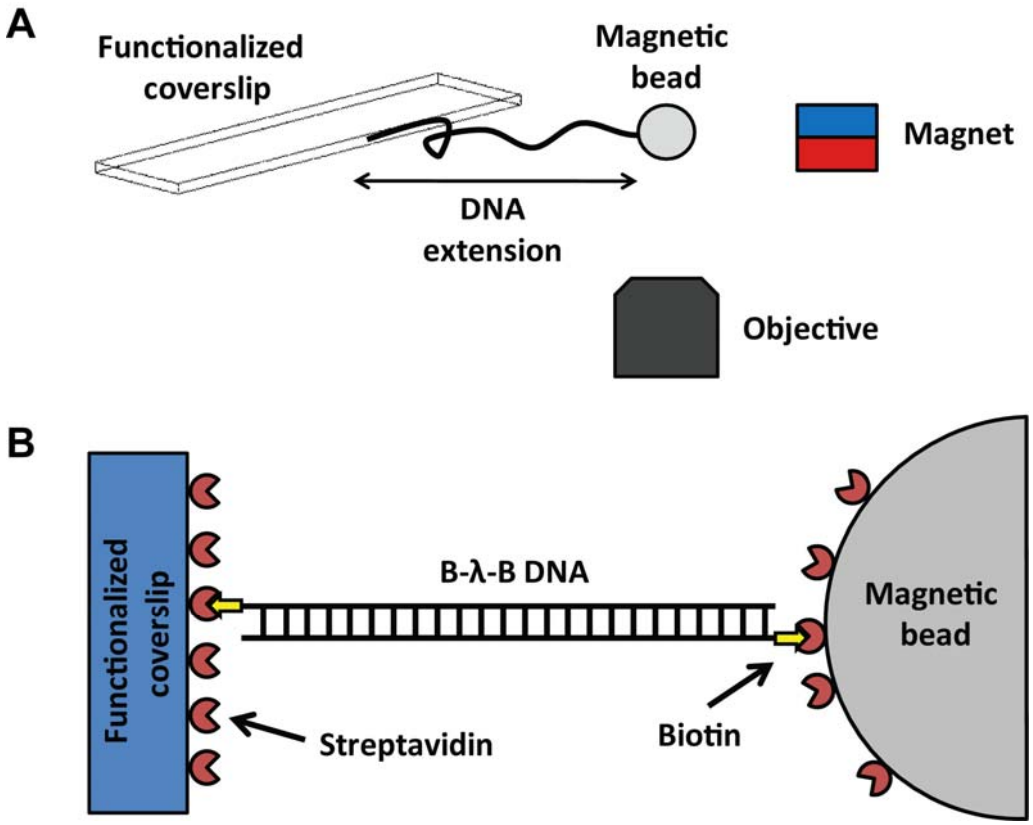

Supplementary Figure S9. Transverse magnetic tweezers setup. (A) The schematic of transverse magnetic tweezers in an inverted microscope setup. (B) The schematic of the DNA tethering using a streptavidin-coated coverslip edge, B-λ-B DNA construct and the streptavidin-coated magnetic bead.

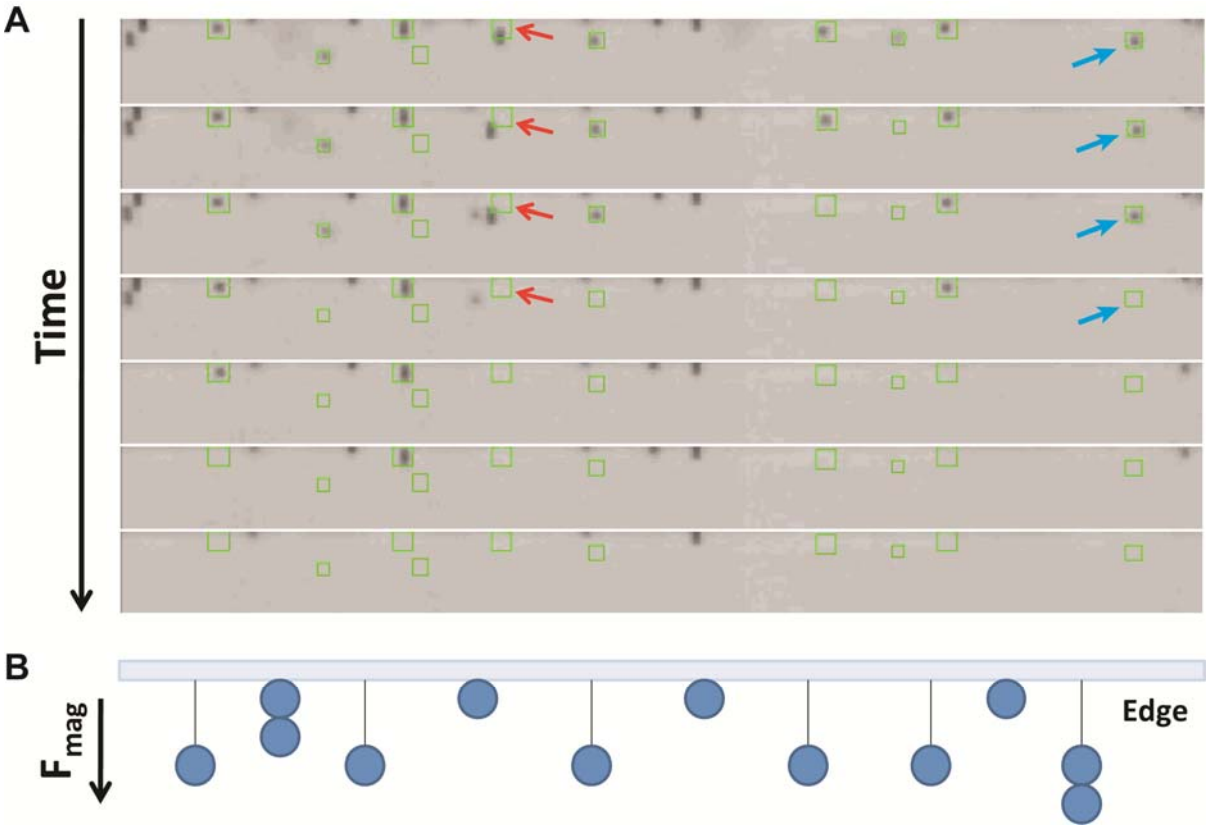

Supplementary Figure S10. High-throughput magnetic tweezers experiment setup and measurements (A) Time-lapsed screenshots of high-throughput magnetic tweezers experiment of DNA tethers cleaving with 1,280 nM DNase I in 500 mM KCl buffer condition. The green boxes are the selected ROIs enclosing DNA tethers. The blue arrows follow the process of a single DNA tether being cut by DNase I resulting in the bead moving away from the screen at frame 5. The red arrows follow the process of a possibly multi-DNA tethered bead where the first DNase I cleaving event resulted in the bead leaving the ROI at frame 2 although it did not leave the screen. This is recorded as a single DNA breakage event. The bead was not traced after frame 2 even though the tether was further cut which resulted in the bead leaving the screen in frame 4. (B) The cartoon schematic of the experimental setup shown in Figure S9A. Due to the geometry of the magnet, stacked magnetic beads will be observed at such high beads density. Some beads will be attached directly onto the edge due to multi-DNA tethering.

References

1. Fu, H., Chen, H., Zhang, X., Qu, Y., Marko, J.F. and Yan, J. (2011) Transition dynamics and selection of the distinct S-DNA and strand unpeeling modes of double helix overstretching. *Nucleic Acids Res*, **39**, 3473-3481.
2. Wang, H., Bash, R., Yodh, J.G., Hager, G.L., Lohr, D. and Lindsay, S.M. (2002) Glutaraldehyde modified mica: a new surface for atomic force microscopy of chromatin. *Biophys J*, **83**, 3619-3625.
3. Bao, Q., Chen, H., Liu, Y., Yan, J., Droge, P. and Davey, C.A. (2007) A divalent metal-mediated switch controlling protein-induced DNA bending. *J Mol Biol*, **367**, 731-740.
4. Liu, Y., Chen, H., Kenney, L.J. and Yan, J. (2010) A divalent switch drives H-NS/DNA-binding conformations between stiffening and bridging modes. *Genes Dev*, **24**, 339-344.
5. Fu, H., Freedman, B.S., Lim, C.T., Heald, R. and Yan, J. (2011) Atomic force microscope imaging of chromatin assembled in Xenopus laevis egg extract. *Chromosoma*.
6. Rivetti, C. and Codeluppi, S. (2001) Accurate length determination of DNA molecules visualized by atomic force microscopy: evidence for a partial B- to A-form transition on mica. *Ultramicroscopy*, **87**, 55-66.
7. Vossepoel, A.M. and Smeulders, A.W.M. (1982) VECTOR CODE PROBABILITY AND METRICATION ERROR IN THE REPRESENTATION OF STRAIGHT-LINES OF FINITE LENGTH. *Computer Graphics and Image Processing*, **20**, 347-364.
8. Yan, J., Skoko, D. and Marko, J.F. (2004) Near-field-magnetic-tweezer manipulation of single DNA molecules. *Phys Rev E Stat Nonlin Soft Matter Phys*, **70**, 011905.
9. Allemand, J.F., Bensimon, D. and Croquette, V. (1996) The elasticity of a single supercoiled DNA molecule (vol 271, pg 1835, 1996). *Science*, **272**, 797-797.
10. Strick, T.R., Allemand, J.F., Bensimon, D., Bensimon, A. and Croquette, V. (1996) The elasticity of a single supercoiled DNA molecule. *Science*, **271**, 1835-1837.
11. Bustamante, C., Marko, J.F., Siggia, E.D. and Smith, S. (1994) Entropic Elasticity of Lambda-Phage DNA. *Science*, **265**, 1599-1600.
12. Marko, J.F. and Siggia, E.D. (1995) Stretching DNA. *Macromolecules*, **28**, 8759-8770.
13. Smith, S.B., Finzi, L. and Bustamante, C. (1992) Direct mechanical measurements of the elasticity of single DNA molecules by using magnetic beads. *Science*, **258**, 1122-1126.